Supplementary Information

A doubly interpenetrated perylene diimide-based zirconium metal-organic framework for selective oxidation of sulfides powered by blue light

Chao Wei,‡[ab] Ming Lu,‡[a] Jing-Jing Li,[a] Ze-Jiu Diao,[a] Guoliang Liu,*[a] Xiao-Qin Liu[a] and Lin-Bing Sun*[a]

[a] State Key Laboratory of Materials-Oriented Chemical Engineering, Jiangsu National Synergetic Innovation Center for Advanced Materials (SICAM), College of Chemical Engineering, Nanjing Tech University, Nanjing 211816, China

[b] College of Science, Jinling Institute of Technology, Nanjing 211169, China

‡ These authors contributed equally to this project.

* Corresponding authors. E-mail: glliu@njtech.edu.cn; lbsun@njtech.edu.cn

1. Chemicals and Reagents

1,6,7,12-Tetrachloroperylene tetracarboxylic acid dianhydride (95%+, Aladdin), 4-Amino-3-methylbenzoic acid (98%+, Adamas), zirconium (IV) chloride ($ZrCl_4$, Sigma-Aldrich), methyl phenyl sulfide and its derivatives (Adamas, 99%), sodium hydroxide (NaOH, Sigma-Aldrich), deuterated chloroform (Adamas, 99.8%D+0.03%TMS), deuterated dimethyl sulfoxide (Adamas, 99.9%D+0.03%TMS) were purchased from corresponding suppliers. Acetic Acid (99%, Adamas), propionic acid (99%, Adamas), methanol (MeOH), dichloromethane (DCM), N, N-dimethylformamide (DMF), deionized water, and 37% concentrated hydrochloric acid (HCl) were purchased as the reagent grade from Sinopharm Chemical Reagent Shanghai Co., Ltd. and 420 nm LED (45 W, from Xuzhou Aijia Electrical Technology) were used for irradiation.

2. Experimental Methods

2.1 Synthesis and characterization of N, N'-bis-(3-methyl-4-benzoic acid)-1, 2, 6, 7-tetrachloropylene-3, 4, 9, 10-tetracarboxylic acid diimide (Me-PDI-COOH)

Me-PDI-COOH was synthesized based on the reported literature[1]. Typically, 1,6,7,12-tetrachloro-3,4,9,10-perylene tetracarboxylic acid dianhydride (1.00 g, 1.89 mmol), 3-methyl-4-aminobenzoic acid (2.86 g, 18.90 mmol) and propionic acid (25 mL) were mixed in a round-bottom flask and stirred under reflux at 160 ^{o}C for 16 h. After the reaction the mixture is cooled to room temperature and the precipitate is filtered. The resulting solid was washed several times with DCM and MeOH (V: V=1:1), the final ligand is obtained and recorded as Me-PDI-COOH. ^{1}H NMR (400 MHz, DMSO-d_6): δ 13.16 (s, 2H), 8.66 (s, 4H), 8.03 (d, 2H), 7.95 (s, 2H), 7.55 (s, 2H), 2.22 (s, 6H). The synthetic route of Me-PDI-COOH can be viewed in Scheme S1.

The purity of Me-PDI-COOH was confirmed using ^{1}H NMR analysis (Fig. S1a), where the single peak at 2.25 was ascribed to the hydrogen atom of the methyl group, and the peaks between 7.5 and 9.0 represented the hydrogen atoms on the aromatic carbon. Additionally, the product was verified through Fourier transform infrared (FT-IR) spectroscopy (Fig. S2), the stretching vibrations of the -OH and C=O present in the carboxylic acid were observed to peak at 3430 and 1683 cm^{-1}, respectively. Moreover, the signals discovered at 2982 and 2913 cm^{-1} correspond to the stretching vibrations of the C-H from the -CH_3 group.

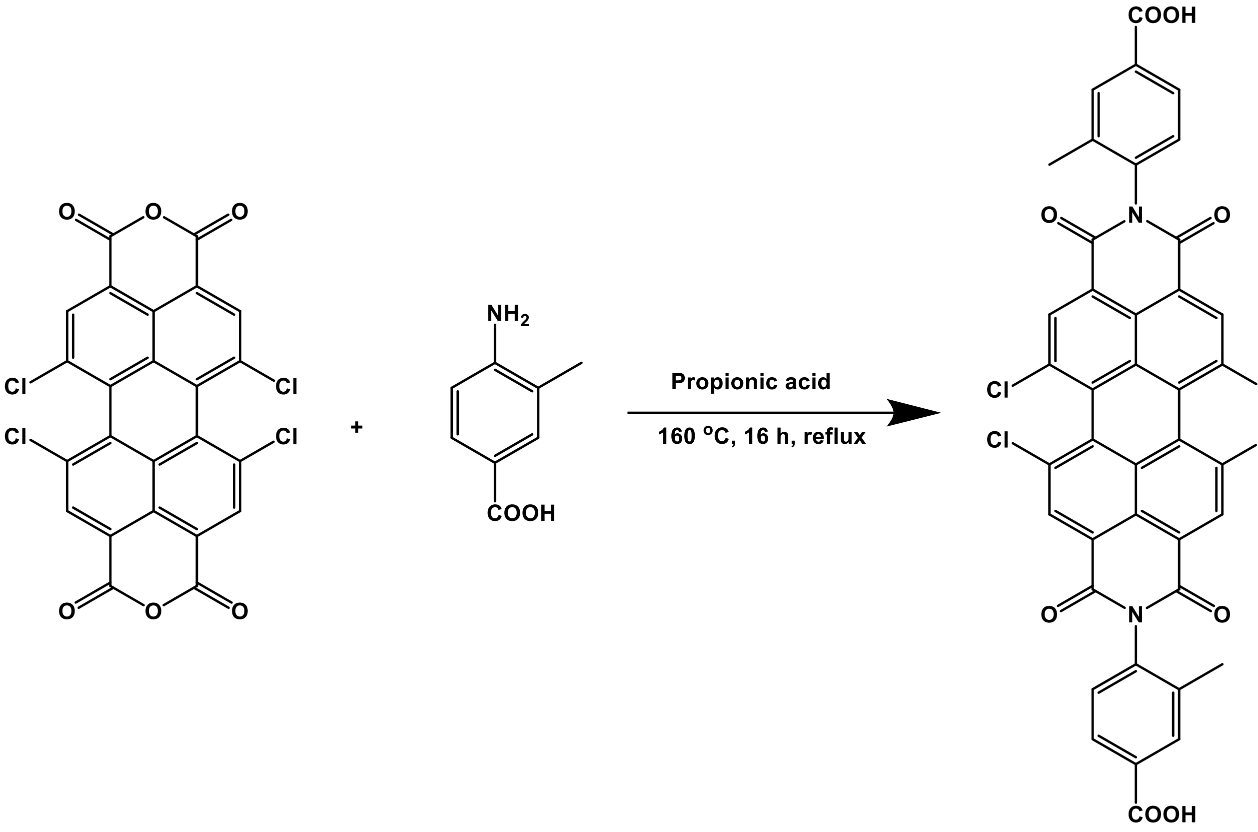

Scheme S1. The synthetic route of Me-PDI-COOH.

2.2 Synthesis of Zr-PDI-Me

The synthesis of Zr-PDI-Me was achieved via a solvothermal process, commencing with the reaction of 0.13 mmol zirconium tetrachloride ($ZrCl_4$) and 0.08 mmol Me-PDI-COOH in a solvent mixture of 16 mL N, N-dimethylformamide (DMF) and 1.25 mL acetic acid. The reaction mixture was maintained at 100 ℃ for a duration of 3 days within a 50 mL sealed vial, followed by gradual cooling to ambient temperature to facilitate the harvesting of red-colored crystals. These crystals were then subjected to a purification step, involving successive washings with DMF and tetrahydrofuran (THF). Subsequent drying under vacuum for 10 hours yielded the final product, Zr-PDI-Me (yield: 47.3%, based on Me-PDI-COOH).

2.3 Digestion of Zr-PDI-Me

5 mg Zr-PDI-Me was dissolved by 1 M sodium hydroxide (NaOH) solution, the obtained flocculent white solid was removed by centrifugation, then the pH of supernatant was

adjusted to 5-6 by 1 M HCl. Next, the collected flocculent red solid was washed with deionized water 3 times before drying in an oven at 100℃. The dried Me-PDI-COOH was detected by ^{1}H NMR, as shown in Fig. S1b.

2.4 The typical procedure for the photocatalytic oxidation of sulfides

To a Pyrex reaction vessel, 0.5 mmol of sulfide was combined with 5 mg of Zr-PDI-Me in 4 mL methanol (MeOH). The reaction was initiated under vigorous stirring and aerated conditions, concurrently exposed to blue light. Upon reaching completion, the mixture was centrifuged to efficiently separate the photocatalyst. The ensuing products were then analyzed by ^{1}H NMR.

2.5 Characterization

^{1}H NMR spectra were recorded at room temperature on a Bruker Avance 400 MHz spectrometer. Chemical shifts are given in ppm with respect to TMS. Fourier transform infrared (FT-IR) spectra were recorded on KBr (1:30, w/w) pellets in the 4000-600 cm^{-1} range using a Perkin-Elmer Spectrum Two FT-IR spectrometer. Powder X-ray diffraction (PXRD) data were collected at 40 kV and 200 mA on a SmartLab 9kW X-Ray diffractometer using Cu-Kα radiation (λ = 1.5418 Å) over 2θ range of 2.0° - 30° at room temperature. Thermogravimetric analyses (TGA) were obtained on a Netzsch TG 209 TG-DTA analyzer with a heating rate of 10 ℃ min-1 under N_2 flow (60 mL/min) from room temperature to 800 ℃. N_2 adsorption-desorption isotherms were carried out using BELSORP-MAX analyzer at 77 K. The Brunauer-Emmett-Teller (BET) surface area was calculated using adsorption data in a relative pressure ranging from 0.05 to 0.30. The pore diameter was calculated from the adsorption branch by using the no-local density functional theory (NLDFT) method. Scanning Electron Microscopy (SEM) experiments were measured on a Hitachi Regulus8100 at 3 kV equipped with an energy dispersive spectrometer (EDS, Oxford Instruments, 80 mm2 detector). UV–vis spectra were obtained on a Shimadzu UV-2600i spectrophotometer and the test range is from 200 to 800 nm. Samples were treated via Pt sputtering before observation. The electron paramagnetic resonance (EPR) experiments were conducted on an electron paramagnetic resonance spectrometer (JEOL, JES-FA300). Single crystal X-ray diffraction analysis was collected on a Bruker APEX-II CCD diffractometer with graphite-monochromated Cu Kα radiation (λ = 1.54178).

Single crystal X-ray diffraction data of Zr-PDI-Me was tested on the Bruker SMART APEX II CCD diffractometer equipped with graphite-monochromatic Mo-Kα radiation (λ = 0.71073 Å). Its scanning method is ϕ/ω, the structure is analyzed by the direct method, and refined on F^2 by the SHELXTL program. The reflection data were corrected by using the SADABS program. Applied anisotropic thermal parameters to non-hydrogen atoms, all hydrogen atoms in organic ligands were counted and added to ideal positions. Due to the inability to identify solvents and ions located in the voids. Therefore, perform SQUEEZE in the PLATON program to remove highly disordered solvents and ions. The relevant crystallographic data were shown in Table S1. Selected bond lengths and angles were listed in Table S2. The CCDC number is 2372570 for Zr-PDI-Me.

Photoelectrochemical measurements were performed on an electrochemical workstation (CHI 660E, CH Instruments Inc., Shanghai) in a standard three-electrode system. The photocatalyst-coated glassy carbon (Φ = 3 cm) was chosen as the working electrode, an Ag/AgCl electrode was applied as a reference electrode, and Pt wire was used as the counter electrode. The electrolyte is a 0.1 M Na_2SO_4 aqueous solution. The samples (10 mg) were dispersed into 1 mL ethanol with 50 μL Nafion mixed solution, and the working electrode was prepared by dropping the suspension onto the surface of the glassy carbon electrode and drying repeatedly (10 μL × 15). The photocurrents were recorded under the 420 nm LED light switching every 20 seconds and 0.5 M Na_2SO_4 solution was chosen as a primer. Electrochemical impedance spectroscopy measurement was performed in the range of 0.1 Hz-100 KHz without light irradiation and the electrolyte was 2.5 mM potassium solution. Mott-Schottky analysis was executed at the frequency of 1000 Hz and the potential range was set between -1 and 1 V based on 0.5 M Na_2SO_4 solution.

2.6 Recycle experiments for the photocatalytic oxidation of sulfides

The photocatalyst, which was recovered by centrifugation, was washed 3 times with methanol to remove the remaining products. It was then dried under vacuum at 60 °C for 2 hours. The recycled photocatalyst was reused in the next cycle under identical conditions.

3. Additional Figures

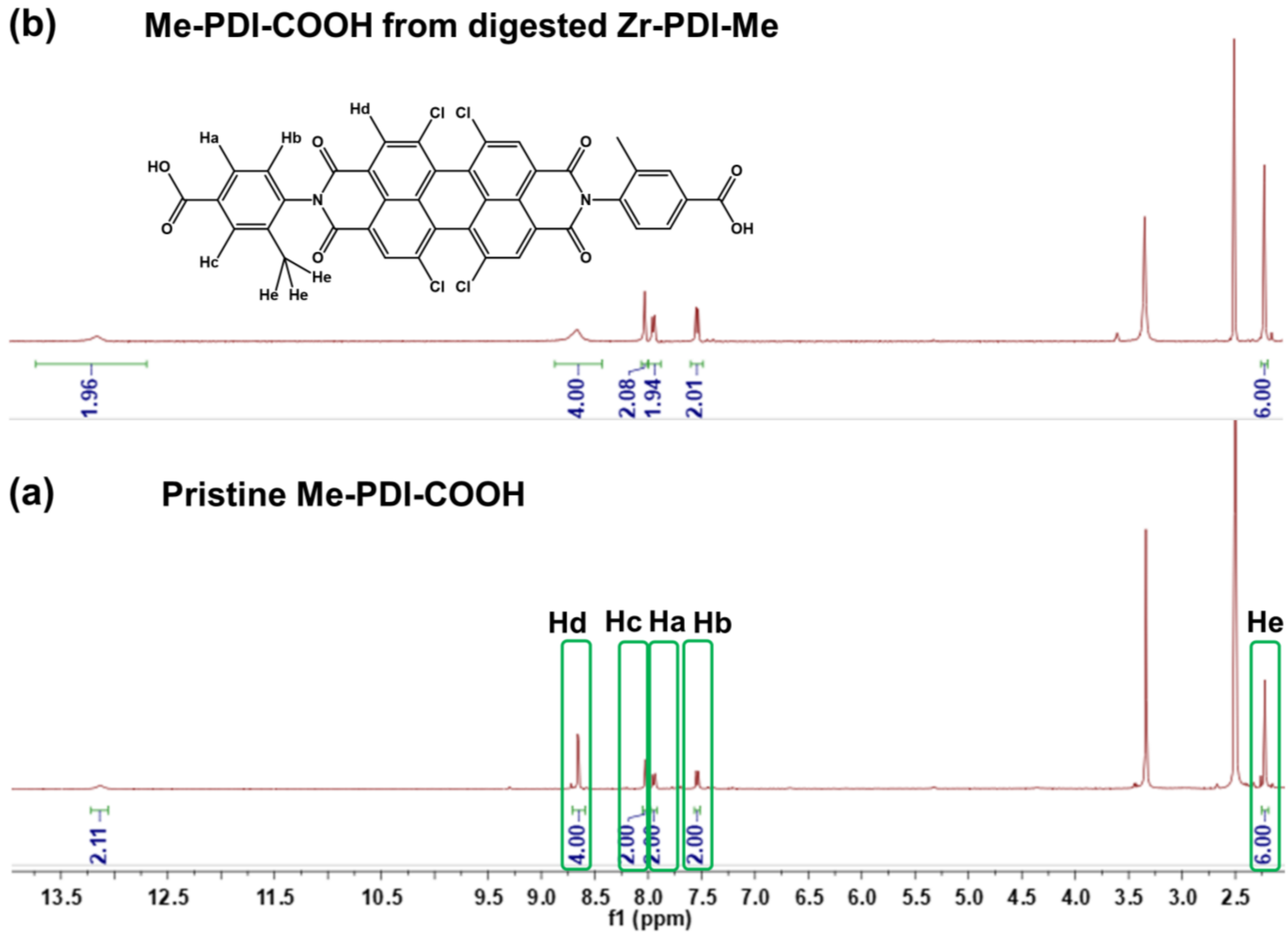

Fig. S1 (a) ^{1}H NMR spectra of pristine Me-PDI-COOH and (b) Me-PDI-COOH from digested Zr-PDI-Me.

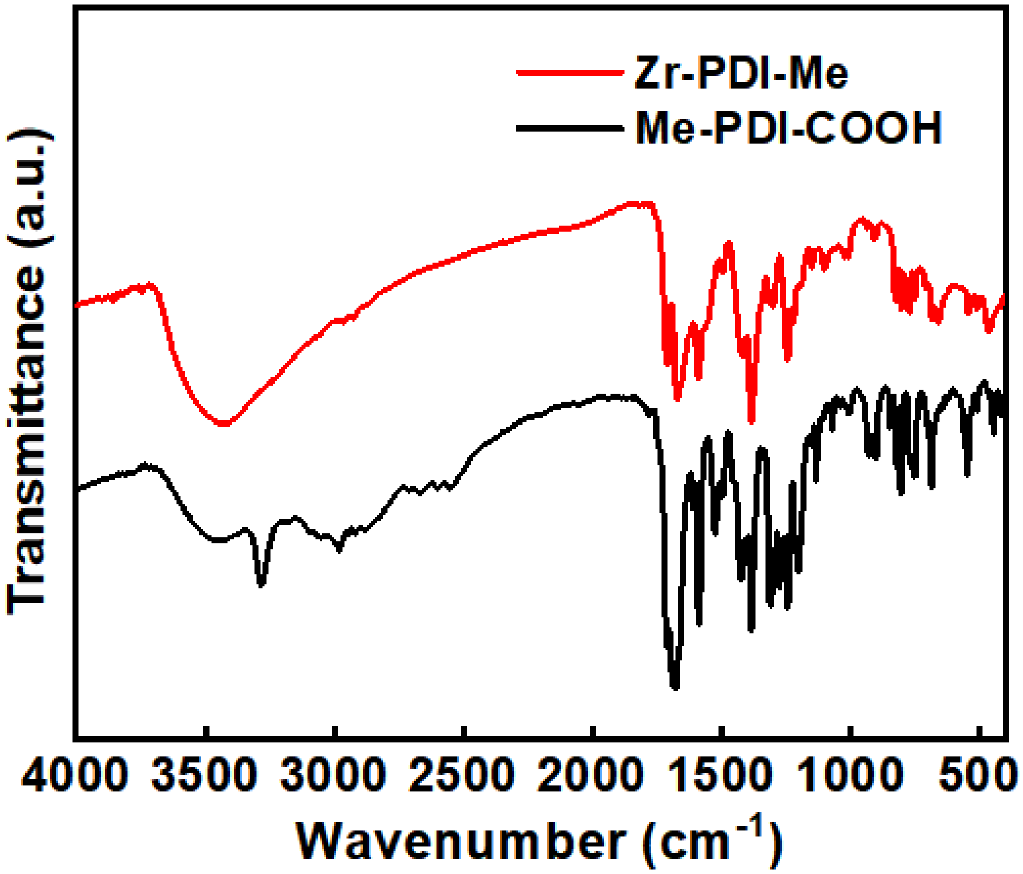

Fig. S2 Full spectra of Me-PDI-COOH and Zr-PDI-Me.

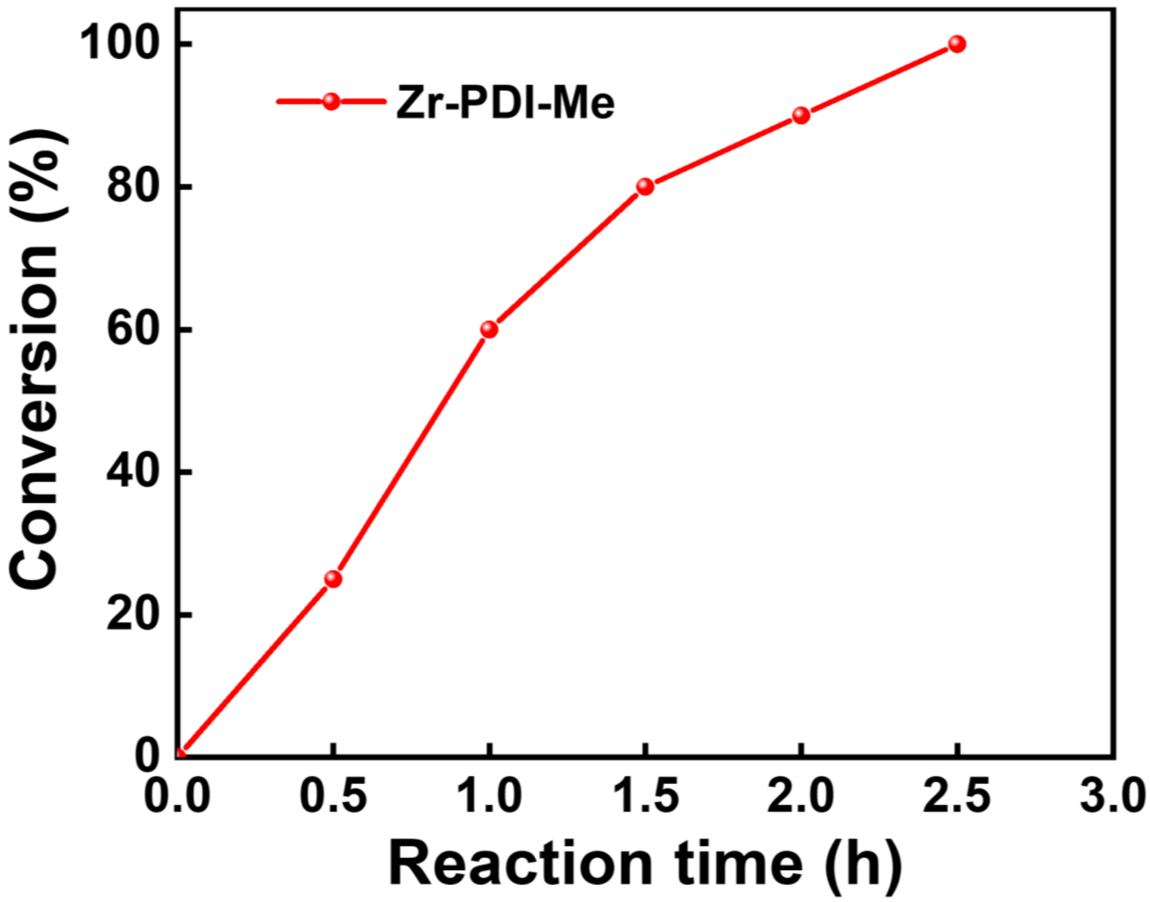

Fig. S3 Conversion of methyl phenyl sulfide in the presence of Zr-PDI-Me.

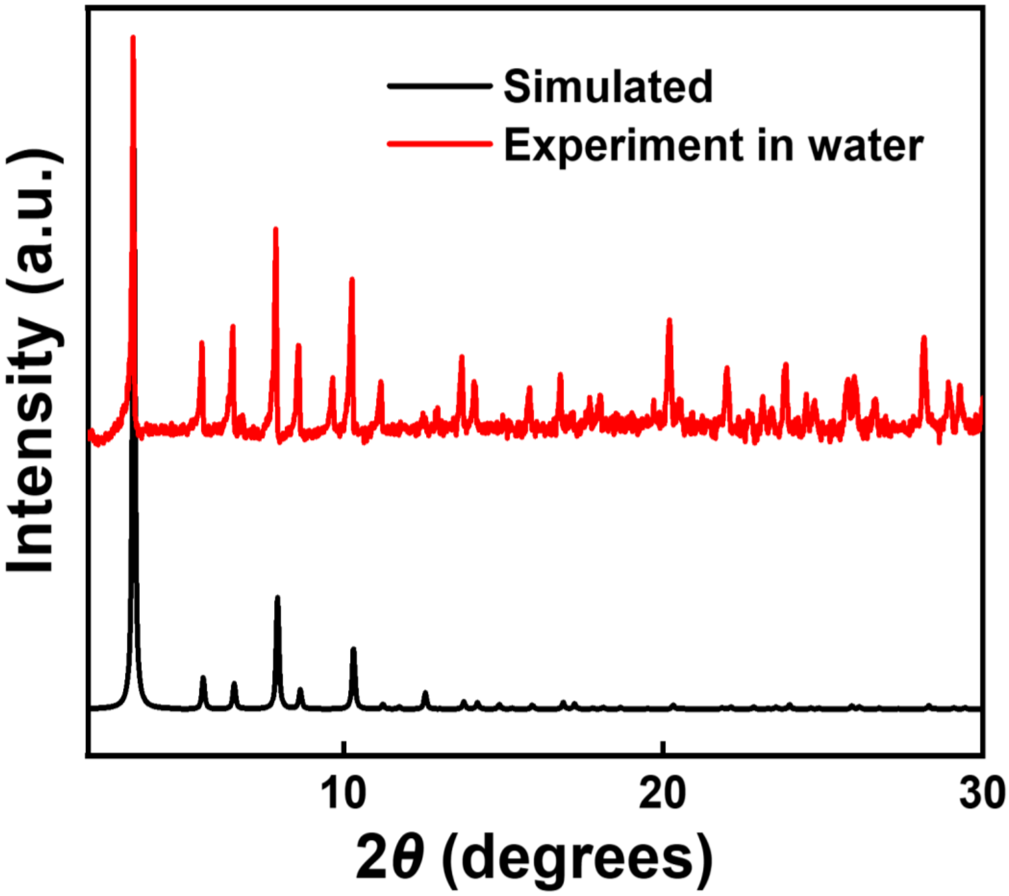

Fig. S4 PXRD analysis of Zr-PDI-Me after 1 run in water.

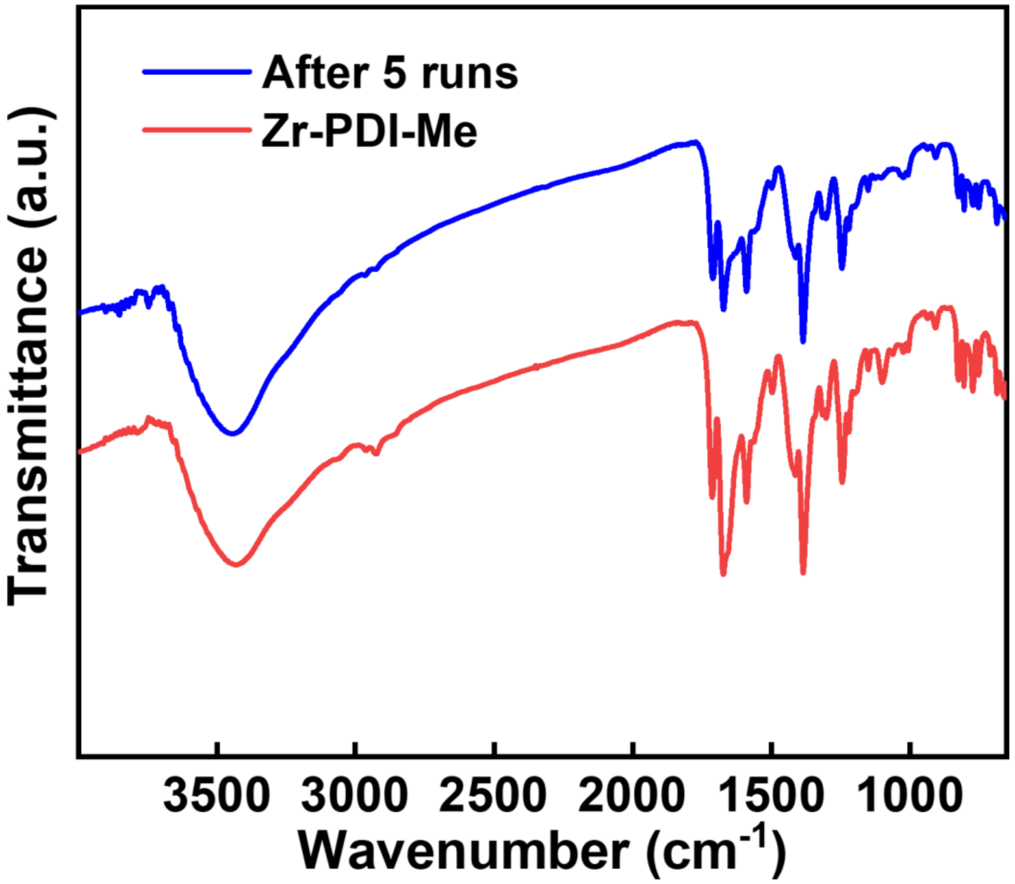

Fig. S5 FT-IR analysis of Zr-PDI-Me after 5 runs.

Table S1 Crystal Data and Structure Refinement for Zr-PDI-Me

Complex	**Zr-PDI-Me**
formula	$C_{114}Cl_{12}N_6O_{28}Zr_3$
fw	2600.26
crystal system	cubic
space group	*Fd-3m*
a /Å	44.5428(13)
b /Å	44.5428(13)
c /Å	44.5428(13)
α **/ °**	90
β **/ °**	90
γ **/ °**	90
V **/Å³**	88376
Z	16
Temperature /K	293
D**calc /g cm⁻³**	1.532
F**(000)**	20384
restrain/parameters	150 / 159
Goodness-of-fit on F^2	1.06
R1, wR2 [I > 2σ(I)]	0.0861, 0.2563
R1, wR2 (all data)	0.0931, 0.2667

$^{a}R_1 = \sum(|F_0| - |F_C|) / \sum|F_0| \cdot \quad wR_2 = \left[\sum w\left(F_0{}^2 - F_C{}^2\right)^2 / \sum w\left(F_0{}^2\right)^2\right]^{0.5}$

Table S2 Selected bond lengths (Å) and angles (o) for Zr-PDI-Me

Zr-O (1)	2.0854(15)	Zr-O (4)	2.214(3)
Zr-O (5)	2.225(3)		
O (1) -Zr-O (1)	99.6(3)	O (4) -Zr-O (4)	119.2(2)
O (5) -Zr-O (5)	103.6(2)	O (1) -Zr-O (4)	81.26(17)
O (1) -Zr-O (5)	71.25(13)	O (4) -Zr-O (5)	74.82(17)

Symmetry transformations used to generate equivalent atoms: *#1 -x+1,y-1/2,-z+1/2；#2 -x+1,-y+1,-z；#3 -x+1, y+1/2, -z+1/2.*

Table S3 Comparison for the photocatalytic performance of Zr-PDI-Me with reported porous materials.

Catalyst	Conditions	T (h)	Yield (%)	Ref.
Zr-MOF-OH	White LED, O_2	8	99	2
PMOF (Ti)	Red LED, O_2	0.75	94	3
Py(4)-TzTz-CMP	Green LED, O_2	2.1	90	4
Tp-COF	Blue LED, O_2	0.5	85	5
TTO-COF	Blue LED, O_2	2	90	6
TTT-COF	Blue LED, O_2	0.5	93	7
TzTz-TA	Blue LED, O_2	0.4	93	8
COF-Tz-2	Blue LED, O_2	0.2	93	9
Zn-AcTA	Blue LED, O_2	9	96	10
h-LZU1	Blue LED, O_2	22	100	11
Ir-Zr-MOFs	Blue LED, O_2	6	100	12
TBPA-COF	Blue LED, Air	1.2	91	13
Hf-NU-1000	Blue LED, Air	0.4	96	14
Yb-MOF	Blue LED, Air	10	99	15
HCP-DiBrAn	Blue LED, Air	3	99	16
Zr_{12}-NBC	Blue LED, Air	10	100	17
Zr-TCA	Blue LED, Air	10	100	18
LCU-600	Blue LED, Air	24	100	19
Zr-PDI-Me	**Blue LED, Air**	**2.5**	**100**	**This work**

References

1. Y.-G. Liu, G. Liu, P. Tan, C. Gu, J.-J. Li, X.-Q. Liu and L.-B. Sun, *Chem. Eng. J.*, 2021, **420**, 130490.
2. Z. Zhao, M. Liu, K. Zhou, L. Guo, Y. Shen, D. Lu, X. Hong, Z. Bao, Q. Yang, Q. Ren, P. R. Schreiner and Z. Zhang, *ACS Appl. Mater. Interfaces*, 2023, **15**, 6982-6989.
3. W. Sheng, H. Hao, F. Huang, F. Zhang and X. Lang, *Chem. Eng. J.*, 2022, **430**, 133071.
4. X. Li, Y. Wang, F. Zhang and X. Lang, *Appl. Catal. B: Environ.*, 2024, **340**, 123190.
5. H. Hao, F. Zhang, X. Dong and X. Lang, *Appl. Catal. B: Environ.*, 2021, **299**, 120691.
6. F. Zhang, H. Hao, X. Dong, X. Li and X. Lang, *Appl. Catal. B: Environ.*, 2022, **305**, 121027.
7. Y. Wang, F. Huang, W. Sheng, X. Miao, X. Li, X.-K. Gu and X. Lang, *Appl. Catal. B: Environ.*, 2023, **338**, 123070.
8. Y. Wang, X. Li, X. Dong, F. Zhang and X. Lang, *J. Colloid Interface Sci.*, 2022, **616**, 846-857.
9. Y. Wang, F. Zhang, F. Huang, X. Dong, B. Zeng, X.-K. Gu and X. Lang, *Appl. Catal. B: Environ.*, 2024, **354**, 124103.
10. P. Tamuly and J. N. Moorthy, *ACS Appl. Mater. Interfaces*, 2024, **16**, 3348-3358.
11. C.-J. Wu, X.-Y. Li, T.-R. Li, M.-Z. Shao, L.-J. Niu, X.-F. Lu, J.-L. Kan, Y. Geng and Y.-B. Dong, *J. Am. Chem. Soc.*, 2022, **144**, 18750-18755.
12. L.-Q. Wei and B.-H. Ye, *ACS Appl. Mater. Interfaces*, 2019, **11**, 41448-41457.
13. F. Zhang, X. Ma, X. Dong, X. Miao and X. Lang, *Chem. Eng. J.*, 2023, **451**, 138802.
14. B. Zeng, W. Sheng, F. Huang, K. Zhang, K. Xiong and X. Lang, *Chem. Eng. J.*, 2023, **474**, 145559.
15. L. Yin, J.-B. Huang, T.-C. Yue, L.-L. Wang and D.-Z. Wang, *Inorg. Chem.*, 2024, **63**, 9109-9118.
16. Z.-J. Diao, G.-Z. Wu, T.-J. Zhang, H.-O. Qi, J.-J. Li, M. Lu, G. Liu, X.-Q. Liu and L.-B. Sun, *J. Mater. Chem. A*, 2023, **11**, 16293-16302.
17. X.-N. Zou, D. Zhang, T.-X. Luan, Q. Li, L. Li, P.-Z. Li and Y. Zhao, *ACS Appl. Mater. Interfaces*, 2021, **13**, 20137-20144.
18. D. Zhang, X.-N. Zou, X.-G. Wang, J. Su, T.-X. Luan, W. Fan, P.-Z. Li and Y. Zhao, *ACS Appl. Mater. Interfaces*, 2022, **14**, 23518-23526.
19. X. Si, Y. Zhang, X. Zhang, X. Pan, F. Wang, X. Shao, Q. Yao, W. Duan, X. Huang and J. Su, *Inorg. Chem.*, 2024, **63**, 4707-4715.